Improving the Characteristics of Phase Change Materials for use in Cooling Bifacial Solar Panels: A Preliminary Study

Sam L. T. Honey[1], Darsh H. Shah[1], Bethan L. Charles[1], Maria Valero[1] and Hind Saidani-Scott[1]

[1] School of Electrical, Electronic and Mechanical Engineering, University of Bristol, Bristol, BS8 1TR, UK (United Kingdom)

Abstract

Effective passive cooling is critical for sustaining the performance and transparency of bifacial photovoltaic modules. This study evaluated three key properties of phase change materials (PCMs) for such applications: degree of supercooling, transmissivity and thermal conductivity. To enhance these properties, three different nucleating agents, zinc oxide (ZnO), graphite and titanium dioxide (TiO_2), were added at different concentrations. ZnO at 0.1 wt% was found to be the best overall, reducing supercooling from 18.5 °C to 2.5 °C, improving conductivity by 37%, and maintaining high transmissivity (91.1% in liquid state). Graphite was most effective at enhancing heat transfer, with a 146% increase at 0.5 wt%, but decreased transmissivity by 96.6%. TiO_2, meanwhile, yielded little thermal benefit and decreased light transmission. This work points to ZnO as the most promising additive for enabling transparent PCM cooling in bifacial modules, leading the way for a cost-effective method to enhance bifacial performance and longevity.

Keywords: bifacial photovoltaic, phase change material, supercooling, thermal conductivity, transmissivity

1. Introduction

Solar energy is the most abundant form of energy on Earth, with 173,000 TW incident on the Earth's surface, around 10,000 times greater than the global energy demand. However, to reach net-zero emissions by 2050, renewable energy capacity needs to triple by 2030 (UNFCCC, 2023). This may not be possible solely by increasing installed capacity, as it requires an exponential increase in the installation of an additional 26% every year. Solar photovoltaics (PV) will become the greatest power capacity out of any renewable energy technology by 2029 (IEA, 2024). Therefore, it is essential to explore other methods to further enhance PV power generation. Among the various PV technologies, bifacial photovoltaics (bPV) have become the dominant type of PV module, accounting for the majority of the market share, as shown in Figure 1.

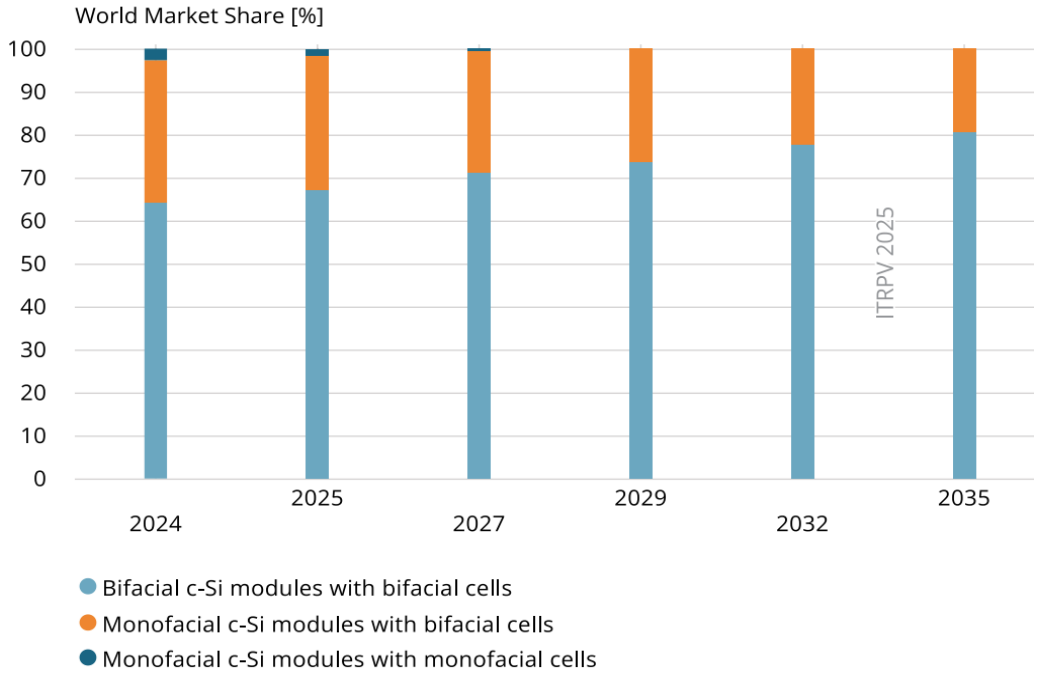

Figure 1: Predicted market share of monofacial and bifacial modules between 2024 to 2035. (Reproduced from Fischer *et al*, 2025)

10.18086/swc.2025.02.17 Available at http://proceedings.ises.org

This is because bPV can absorb light on both sides of the panel, thus achieving higher power outputs than monofacial panels for a given area (Gu *et al*., 2020). Cooling bPV modules increases their efficiency and reduces cell degradation. However, unlike monofacial technology, bPV require transparent cooling solutions. The use of phase change materials (PCMs) is a promising passive cooling method. Honey *et al*. (2023) have shown that Calcium Chloride Hexahydrate ($CaCl_2 \cdot 6H_2O$, CCH) can be used to improve the efficiency of bPV by up to 10.7%. However, CCH tends to supercool and has low thermal conductivity, a common problem with PCMs (Sharma and Sagara, 2005). Supercooling occurs when the material must overcome a large Gibbs free energy barrier for homogeneous nucleation, thus requiring lower temperatures to initiate crystallisation (Zhao *et al*., 2020). The addition of nucleating agents reduces the solid-liquid interfacial energy, which reduces the free energy barrier by providing more surfaces for heterogeneous nucleation to occur (Adachi *et al.*, 2014). Nucleating agents often have higher thermal conductivities and can also increase the overall thermal conductivity of the mixture. However, the effect on the transmissivity of the mixture is not typically considered when searching for the best nucleating agent. Therefore, this work measured the effects of adding different nucleating agents on the degree of supercooling, thermal conductivity and transmissivity of the resulting mixtures. Furthermore, as the rate of cooling can also affect the degree of supercooling, the effect of the rate of cooling on the transmissivity of the chosen mixture was investigated.

2. Methodology

2.1 Material Selection and Preparation

To both decrease the degree of supercooling and increase the thermal conductivity of CCH PCM, the primary criterion for selecting nucleating agents was thermal conductivity. Whilst $BaCO_3$, K_2CO_3 and $SrCl_2.6H_2O$ have all been shown to be effective nucleating agents for CCH, their thermal conductivities are relatively low (Sutjahja *et al*., 2016). Graphite has a very high in-plane thermal conductivity, up to 1910 W/mK and has also been previously used to enhance the thermal properties of salt hydrate PCMs (Klemens and Pedraza, 1994). ZnO also has a relatively high thermal conductivity, ranging from 37 to 49 W/mK at room temperature (Wu *et al.* 2016). Furthermore, ZnO has been used to reduce the supercooling of other salt hydrates, including zinc nitrate hexahydrate (Kumar *et al.*, 2018). Finally, TiO_2 has already been shown to decrease the degree of supercooling in salt hydrates, including in the eutectic mixture of 90% calcium chloride hexahydrate and 10% magnesium chloride hexahydrate, as well as increase the thermal conductivity of this mixture by as much as 48.1% (Wang *et al.*, 2022). The concentrations of each nucleating agent tested were: 0.1 wt% TiO_2, 0.1 wt% graphite, 0.5% wt graphite, 0.1 wt% ZnO, 0.5 wt% ZnO and 1.0 wt% ZnO. For both the supercooling and transmissivity experiments, the samples were put inside acrylic containers of 100x100x5mm and for the conductivity experiment, containers of 100x100x10mm. The mass of the CCH was measured and then melted using a hotplate set to 40°C. Then, for each concentration, the nucleating agent was measured and added to the molten CCH, and the mixture was stirred using stir bars. Once uniformly distributed through the mixture, the samples were added to the containers and sealed using clear silicone.

2.2 Supercooling Characterisation

A TC-08 Pico data logger and a K-type thermocouple were used to measure the temperature of the samples inside the containers. The samples were cooled inside a temperature-controlled box, (Figure 2).

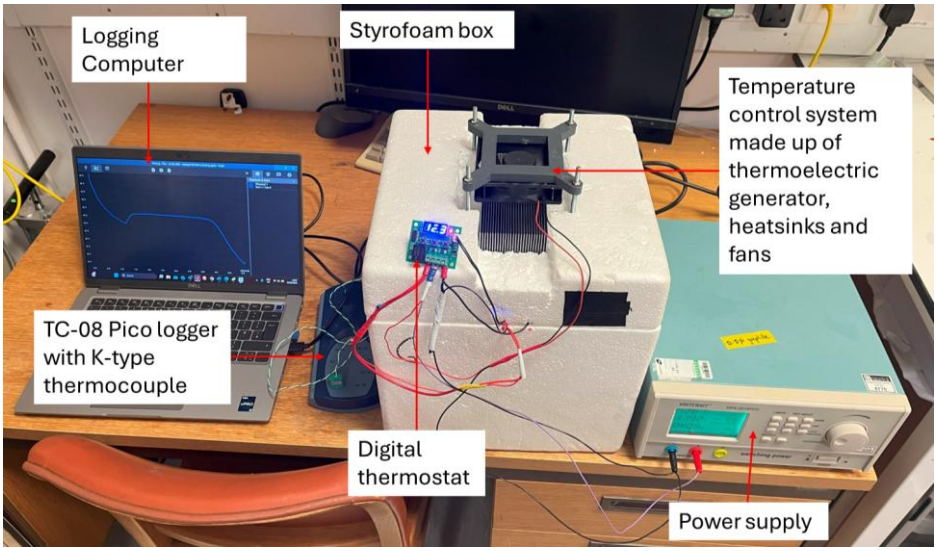

Figure 2: The experimental setup to measure the degree of supercooling.

The temperature-controlled box consisted of a Styrofoam box with a wall thickness of 50 mm, a TEC1-12706 thermoelectric generator (TEG), two heat sinks and two fans. The TEG was sandwiched between the two heat sinks, with the cold side facing inward and the hot side facing outward. One fan was attached to the heat sink inside the box to circulate air, creating a more uniform environment. The other fan was then used on the external heat sink to dissipate heat away from the system. The voltage across the TEG was then controlled using a W1209 digital thermostat, where the temperature difference between the faces is directly proportional to the voltage. A typical crystallisation curve of a material that is prone to supercooling is shown in Figure 3.

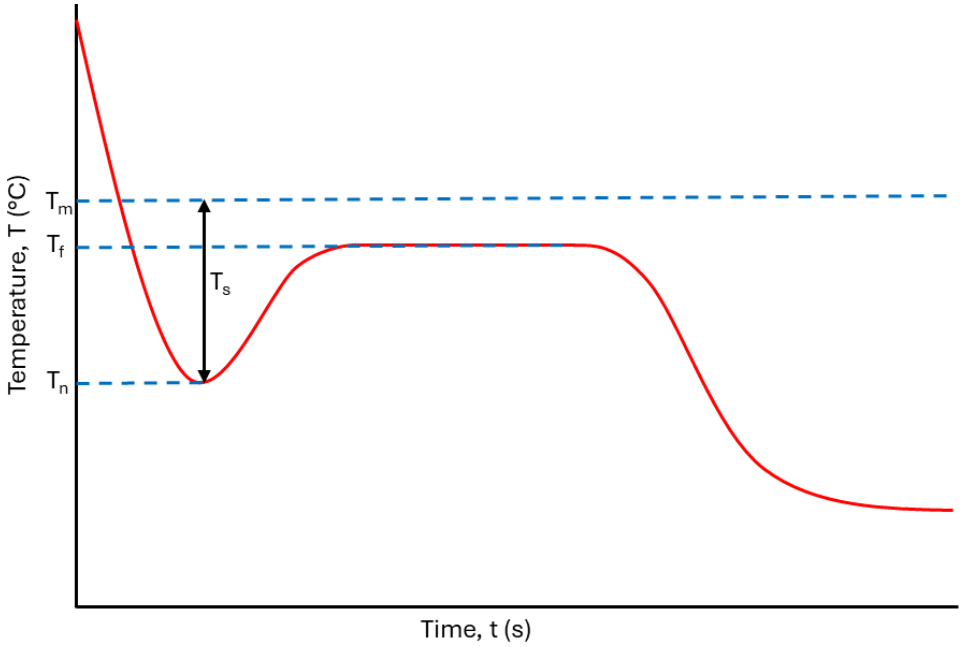

Figure 3: Typical crystallisation curve for a material that supercools.

The degree of supercooling, T_s, is given by the difference between the melting temperature, T_m, and the temperature at which nucleation starts, T_n. It is important to note that the freezing temperature, T_f, can be lower than the melting temperature. This occurs when the heat removal from the system equals the latent heat of solidification, either due to a high rate of heat removal or poor crystallisation kinetics (Safari *et al.*, 2017).

2.3 Thermal Conductivity

A 100x100x10mm acrylic container of CCH was heated to a steady 55 °C and insulated on all sides to ensure only one-dimensional heat transfer. The temperature at the top and bottom of the samples was measured using K-type thermocouples, (Figure 4).

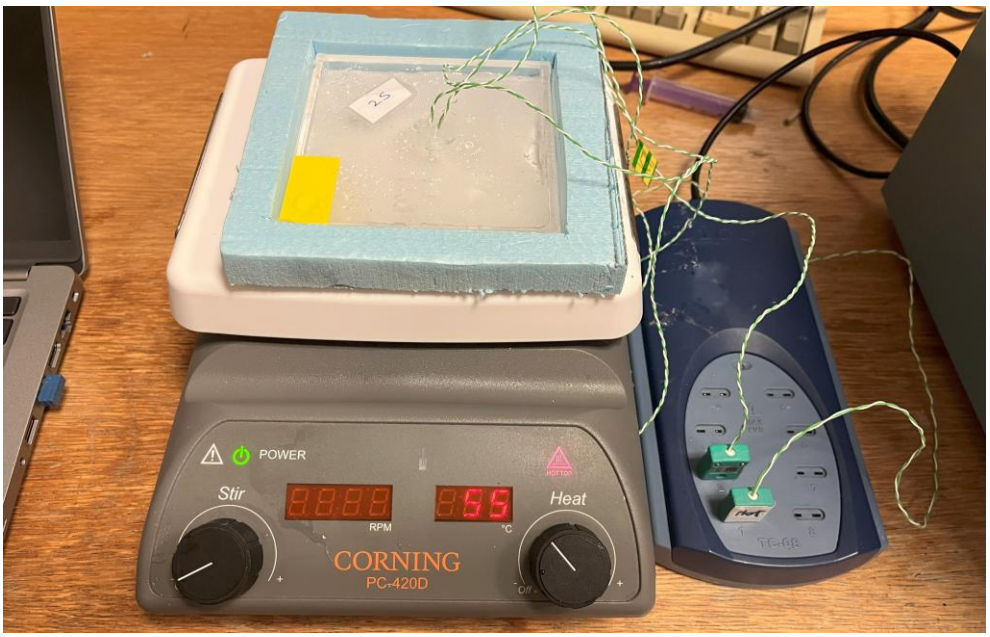

Figure 4: The experimental setup for measuring thermal conductivity.

As the heat source could only be set to a constant temperature and not a constant heat flux, the control sample with pure CCH, with known thermal conductivity (Tyagi and Buddhi, 2008) was used to estimate the change in the power output of the hot plate as the temperature of the samples increased. This was done using Fourier's Law, (eq. 1),

$$\dot{Q} = -\frac{k\,A\,(T_t - T_b)}{dx} \qquad \text{(eq. 1)},$$

where $\dot{Q}$ is the rate of heat transfer, k the thermal conductivity, A the area, T_t the temperature at the top of the sample in the container, T_b the temperature at the bottom of the sample in the container and dx the distance between the thermocouples. It was then assumed that the rate of heat transfer for all the samples was the same for given temperature differences between the hot plate and the bottom of the sample, as identical acrylic containers were used. Thermal conductivities of each sample could then be found from eq. 1. Due to the uncertainty of the heat flux of the hotplate, the results should be interpreted as relative change in thermal conductivities due to the nucleating agents and not absolute values.

2.4 Transmissivity

For the transmissivity experiments, the samples were placed under a 1000 W tungsten-halogen lamp that approximated the solar spectrum. Irradiance was measured using an Extech SP505 PV meter, (400 and 1100nm). at a set distance through the samples, as seen in Figure 5.

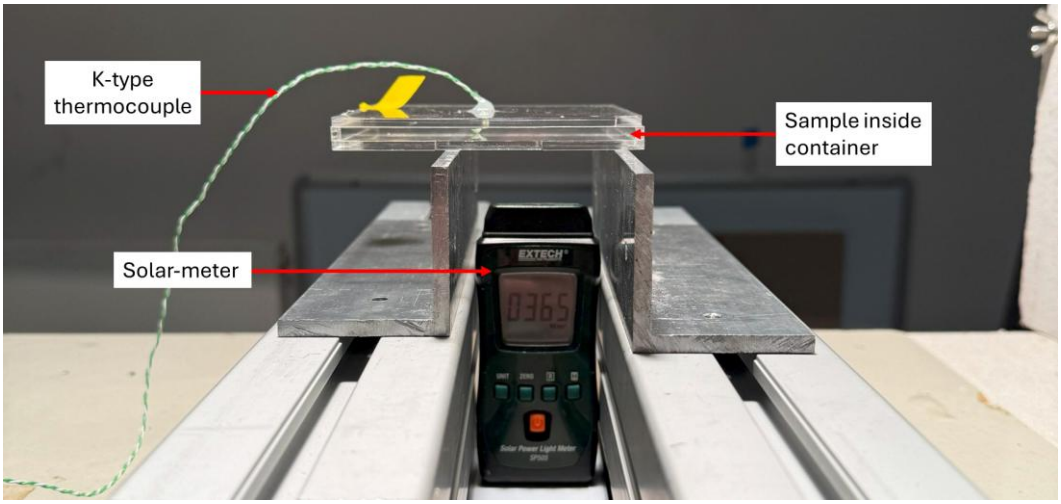

Figure 5: The experimental setup to measure inline transmission.

The irradiance with no sample was 415W/m^2. The transmissivity was measured through averaging the transmission through four different points in the sample below and above the melting point to account for both in the solid and liquid phases.

2.5 Cooling rate

The effect of cooling rate on the average crystal size and, in turn, how that affects the transmissivity of the material was investigated. For this, three 0.1 wt% ZnO samples were fully melted and heated to 40°C, then left to freeze in three different conditions: one at room temperature (25°C), the second in a fridge at 8°C, and the third in a freezer set to -5°C. These were chosen to simulate a full range of environmental freezing conditions in the UK, from a warm summer's night to a cold winter's night. The samples were then left to crystallise overnight. Then, using the same method discussed in Section 2.4, the transmissivity of each sample was calculated. The average grain size of each sample was calculated using back lit photographs, the software ImageJ, and a ruler used to calibrate the scale.

3. Results and Discussion

Firstly, looking at the degree of supercooling, the temperatures during the cooling of each sample can be seen in Figure 6. From this, the degree of supercooling was calculated and summarised in Table 1. The results from the thermal conductivity and transmissivity experiments are also summarised in Table 1.

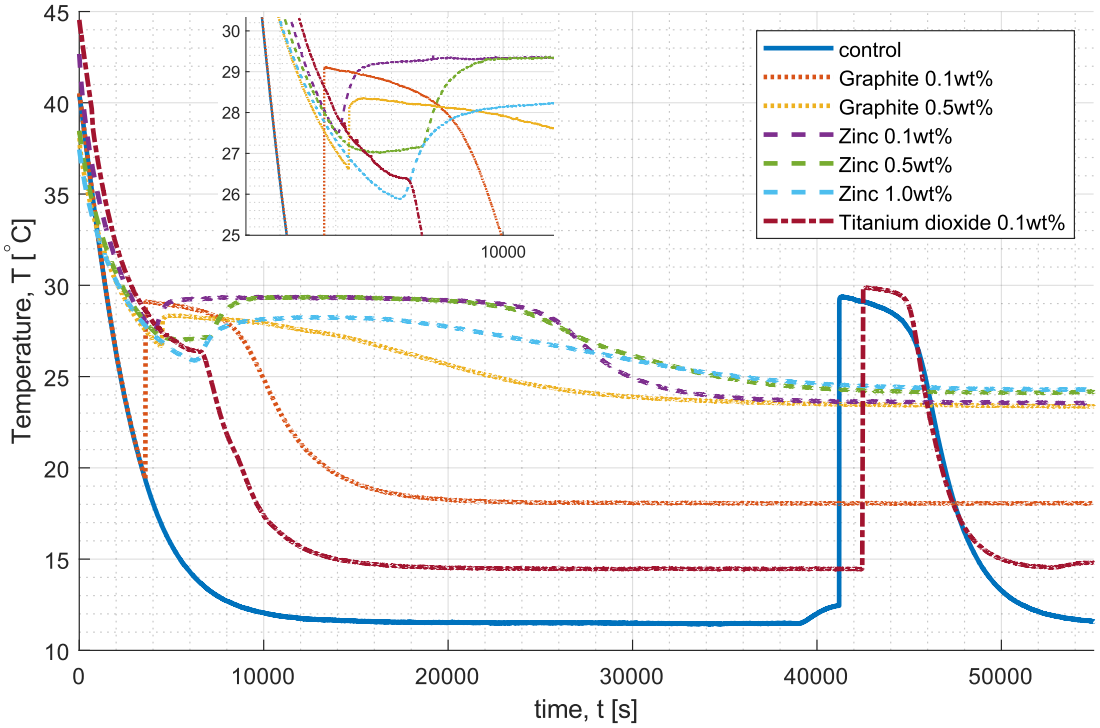

Figure 6: Sample temperature on cooling a CCH control and CCH doped with graphite, ZnO and TiO_2 as nucleating agents, allowing the degree of supercooling to be calculated. The insert shows a zoomed view of the nucleation points of the best performing samples.

CCH doped with 0.1 wt% ZnO reduced the degree of supercooling the most, from 18.5°C (for the control) down to only 2.5 °C, closely followed by the 0.5 wt% of graphite, 0.5 wt% ZnO and 1.0 wt% ZnO, reducing supercooling to 3.4 °C, 4.2 °C and 4.5 °C, respectively. The TiO_2 had very little effect on the degree of supercooling.

The degree of supercooling decreases with increasing graphite concentration but increases with increasing ZnO concentration. This can be explained due to the need for different optimal concentrations for different nucleating agents (Fashandi and Leung, 2018; Cui *et al.*, 2023). As the concentration increases, the likelihood of agglomeration increases, decreasing the number of nucleation sites. Fashandi and Leung also demonstrated that as the particle size of the nucleating agent decreased, the degree of supercooling decreased accordingly. Particle size was not controlled across the different nucleating agents in this study, but it should be explored further in future research.

Only the TiO_2 sample froze at the melting temperature of 30°C, suggesting that the supercooling was due to a slow rate of crystal growth (Safari *et al.*, 2017). However, this may also be due to a high heat transfer rate due to large temperature differences between the air in the temperature-controlled box and the samples. Increased cooling rates increase the degree of supercooling (Taylor *et al.*, 2016). To improve upon the methodology, a more complex control system that utilises both the sample's temperature and the box's temperature could be created to minimise the rate of heat transfer and thus the degree of supercooling.

Another thing to note from Figure 6 is that the ZnO, TiO_2 and the 0.5 wt% graphite samples cooled at a slower rate than the control and 0.1 wt% graphite samples. It is proposed this is due to nucleation occurring away from the temperature sensor resulting in the latent heat release slowing cooling. This was supported by taking infrared photos of the 0.1 wt% ZnO samples during nucleation, as shown in Figure 7.

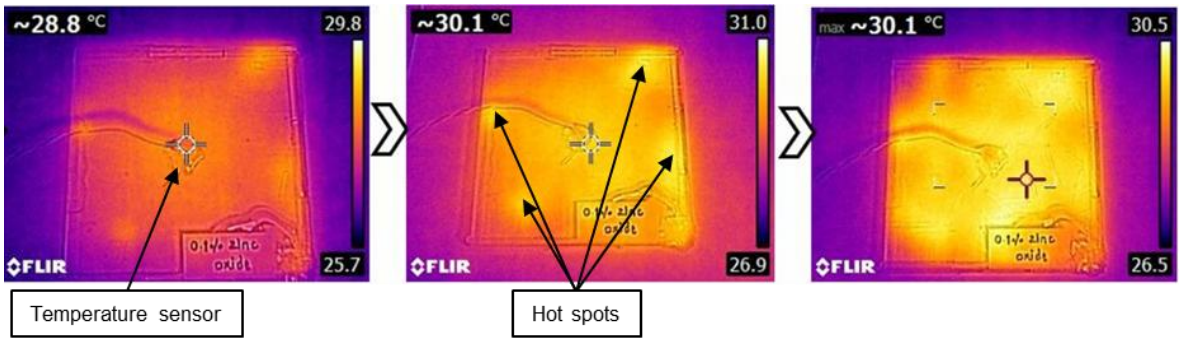

Figure 7: Infrared images showing temperature rises from points of nucleation.

Figure 7 shows hot spots forming away from the temperature sensor, and at higher temperatures than the readings

of the thermocouple. This could be due to non-uniformity in the distribution of the nucleating agent causing nucleation to occur quicker at some points. Another observation of Figure 6 is that all except the ZnO-doped samples have a steep rise in temperature after the point of nucleation, suggesting that the ZnO lowers the thermal diffusivity of the CCH. This is further exemplified by the fact that ZnO-doped CCH have the longest freezing times. Two possible explanations for this would be a decrease in thermal diffusivity or an increase in latent heat capacity. Thermal diffusivity is proportional to the thermal conductivity and inversely proportional to the specific heat capacity. From examining Table 1, we can see that the ZnO samples all increase the thermal conductivity. Suggesting that the specific heat or latent heat capacity has increased. However, it could also be due to an uneven distribution of the nucleating agent. To further investigate the cause of uneven freezing and prolonged freeze times, the effects on specific heat and latent heat capacity should be measured using differential scanning calorimetry, allowing for the calculation of thermal diffusivity. Finally, X-ray diffraction could be conducted on the samples to see if there is an effect on the microstructure of the crystals.

Table 1: Thermal and optical properties of CCH and CCH doped with graphite, ZnO and TiO_2.

Sample	Degree of supercooling, T_s (°C)	Increase in Thermal Conductivity (%)	Transmission through solid (%)	Transmission through liquid (%)
Control (CCH)	18.5	-	57.3	91.2
Graphite 0.1 wt%	10.6	+114	23.2	16.0
Graphite 0.5 wt%	3.4	+146	8.19	3.13
ZnO 0.1 wt%	2.5	+37.4	48.0	91.1
ZnO 0.5 wt%	4.2	+78.9	46.7	73.4
ZnO 1.0 wt%	4.5	+106	34.8	45.8
TiO_2 0.1 wt%	15.5	+14.1	41.8	30.2

The thermal conductivity of CCH increases with the addition of each nucleating agent and with the increasing concentration of the nucleating agents. The greatest increase is observed in the graphite samples, with a 146% increase for 0.5 wt% graphite-doped CCH. Furthermore, 0.1wt% ZnO-doped CCH, which exhibited the greatest reduction in degree of supercooling and the highest transmissivity, also showed a significant increase in thermal conductivity of 37% from the control. From this, an alternative explanation for the rapid increase in temperature of the graphite samples is that it is due to the significant increase in thermal conductivity. Additionally, the rapid increase in temperature observed in the TiO_2-doped CCH and pure CCH samples may be attributed to the high degree of supercooling present. This is typical behaviour in highly supercooled systems, where a sudden and localised nucleation event leads to a fast release of latent heat, quickly raising the temperature and completing the phase change (Xu *et al.*, 2017).

All temperature measurements were made using the TC-08 Pico data logger and K-type thermocouples, the total uncertainty of which can be calculated as the sum of ± 0.2% of the reading and ± 2°C. This uncertainty is comparable to the temperature differences measured for the thermal conductivities. One improvement would be to use T-type thermocouples for future testing for higher accuracy. Furthermore, the temperature difference could be increased by using the TEG cooling system to cool one side of the sample.

When examining the transmissivity results in Table 1, the first thing to note is that the ZnO-doped CCH exhibited the highest degree of transmissivity, achieving 91.1% at a 0.1 wt% concentration compared to 91.2% for the pure liquid CCH. At low concentrations, the ZnO appeared to dissolve in the CCH, but it is unclear whether it formed a solution or was a fine colloidal suspension. Due to graphite having high absorbance in the visible spectrum, the graphite-doped CCH had particularly low transmissivity at only 3.1% for the liquid 0.5 wt% graphite sample. Interestingly, the transmissivity for the graphite-doped and TiO_2-doped samples increased when solid, unlike the control and ZnO-doped CCH samples, which decreased. This was because, when liquid, the nucleating agents were evenly distributed throughout the samples. However, when frozen, the graphite and TiO_2 accumulated more heavily in the grain boundaries of the CCH, allowing more light to pass through each crystal, as seen in Figure 8.

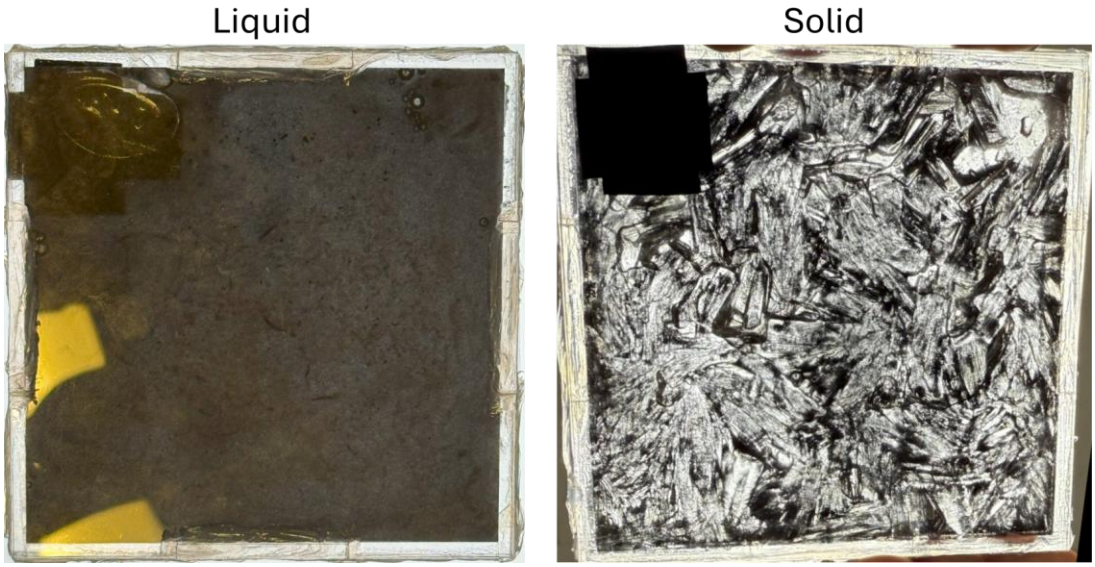

Figure 8: Comparison photos of 0.5 wt% graphite-doped CCH when solid and liquid.

When comparing the transmissivity between liquid and solid CCH, a significant drop occurs during solidification, decreasing from 91.2% to 57.3%. These values are comparable to those in the literature, where Xie *et al.* (2019) found, that the transmissivity of liquid CCH varied between 80% and 100% between 250 and 1100 nm. Moreover, Kalidasan *et al.* (2023) determined the transmissivity of CCH to be 22.6%. Whilst Kalidasan *et al.* (2023) does not explicitly state whether this result was for solid or liquid CCH, there are images of solid CCH when discussing the microstructure seen under a microscope. However, there is still a significant difference between the results, which may be due to differences in how the CCH was prepared. It was hypothesised that this may be due to different cooling rates affecting the grain size of the crystal and thus the transmittance. When exposing the samples to greater temperature differences and increasing the cooling rate, the size of the crystals decreased, as seen in Figure 9. Furthermore, as the average crystal size decreased, transmission increased, as seen in Table 2.

Figure 9: Crystal grain size of 0.1 wt% Zn0-doped CCH for samples cooled at (a) 25 degrees (b) 8 degrees and (c) -5 degrees.

Table 2: Average crystal size and transmissivity according to ambient freezing temperature.

Cooling Temperature (°C)	Average Crystal Area (mm^2)	Transmission through solid (%)
25	72.0	48.0
8	35.6	53.7
-5	10.7	56.7

The precise mechanism by which transmission increases as grain size decreases remains uncertain; a possible explanation is that larger grains deflect more light due to directional scattering, thus reducing in-line transmittance. This should be further investigated using an integrating sphere to measure how the total (hemispherical) transmittance and reflectance vary with the grain size. As the solar meter had a relatively high uncertainty of ± 10 W/m^2, future work should measure the inline transmission using UV-Vis spectroscopy to both improve the accuracy as well as determine how the transmission also varies with wavelength.

4. Conclusion

This preliminary study demonstrates that nucleating agents have a significant impact on the thermal and optical properties of CCH. Graphite provided strong conductivity enhancement, increasing by 146%, and reduced the degree of supercooling to 3.4 °C, but decreased the transmissivity by 96.6%. TiO_2 gave limited improvements with the thermal conductivity only increasing by 14.1% while light transmission was decreased by as much as 66.9% and the degree of supercooling remained high at 15.5 °C. ZnO at 0.1 wt% offered the most balanced performance: the lowest

supercooling of 2.5 °C, moderate conductivity enhancement, increasing by 37.4%, and maintained a high transmissivity of 91.1% when liquid and 48.0% when solid. Future work will investigate the stability of the mixtures of repeated thermal cycling, as well as performing differential scanning calorimetry to assess the effect of the nucleating agents on the latent heat capacity and specific capacity. Finally, the total (hemispherical) transmittance and reflectance should be measured using an integrating sphere.

5. References

Adachi, T., Daudah, D., Tanaka, G., 2014. Effects of supercooling degree and specimen size on supercooling duration of erythritol. Isij International. 15;54(12):2790-5.

Cui, W., Guo, T., Xinhui, Y., Ma, H., Liang, D. and Dong, J., 2023. Experimental study on supercooling and heat transfer performance during the solidification of sodium acetate trihydrate composites. Solar Energy Materials and Solar Cells, 250, p.112098.

Fashandi, M. and Leung, S.N., 2018. Sodium acetate trihydrate-chitin nanowhisker nanocomposites with enhanced phase change performance for thermal energy storage. Solar Energy Materials and Solar Cells, 178, pp.259-265.

Fischer, M., Woodhouse, M., Brammer, T. and Baliozian, P., 2025. International technology roadmap for photovoltaic (ITRPV) 2024 Results, Available at: https://www.vdma.org/international-technology-roadmap-photovoltaic, [Accessed 9th October 2025]

Gu, W., Ma, T., Ahmed, S., Zhang, Y. and Peng, J., 2020. A comprehensive review and outlook of bifacial photovoltaic (bPV) technology. Energy Conversion and Management, 223, p.113283.

Honey, S.L.T., Saidani-Scott, H., Coopey, H., Arkell, T., Cooke-Flores, A., Abdelhamid, A., 2023. Feasibility of Using Phase Change Material Calcium Chloride Hexahydrate to Improve the Efficiency of Bifacial Photovoltaic Modules via Passive Cooling. 2023 IEEE International Conference on Energy Technologies for Future Grids (ETFG), pp. 1-6, doi: 10.1109/ETFG55873.2023.10407975.

IEA, 2024. Renewables 2024, Available at : https://www.iea.org/energy-system/renewables/solar-pv, [Accessed: 14th October 2025]

Kalidasan, B., Pandey, A.K., Saidur, R., Tyagi, S.K. and Mishra, Y.K., 2023. Experimental evaluation of binary and ternary eutectic phase change material for sustainable thermal energy storage. Journal of Energy Storage, 68, p.107707.

Klemens, P.G. and Pedraza, D.F., 1994. Thermal conductivity of graphite in the basal plane. Carbon, 32(4), pp.735-741.

Kumar, N., Banerjee, D. and Chavez Jr, R., 2018. Exploring additives for improving the reliability of zinc nitrate hexahydrate as a phase change material (PCM). Journal of Energy Storage, 20, pp.153-162.

Liu, Y., Li, X., Xu, Y., Xie, Y., Hu, T. and Tao, P., 2024. Carbon-enhanced hydrated salt phase change materials for thermal management applications. Nanomaterials, 14(13), p.1077.

Safari, A., Saidur, R., Sulaiman, F.A., Xu, Y. and Dong, J., 2017. A review on supercooling of Phase Change Materials in thermal energy storage systems. Renewable and Sustainable Energy Reviews, 70, pp.905-919.

Sharma, S.D., Sagara, K., 2005. Latent heat storage materials and systems: a review. International journal of green energy. 2(1), 1-56

Sutjahja, I.M., AU, S.R., Kurniati, N., Pallitine, I.D. and Kurnia, D., 2016, August. The role of chemical additives to the phase change process of CaCl2. 6H2O to optimize its performance as latent heat energy storage system. In Journal of Physics: Conference Series (Vol. 739, No. 1, p. 012064). IOP Publishing.

Taylor, R.A., Tsafnat, N. and Washer, A., 2016. Experimental characterisation of sub-cooling in hydrated salt phase change materials. Applied Thermal Engineering, 93, pp.935-938.

Tyagi, V.V. and Buddhi, D., 2008. Thermal cycle testing of calcium chloride hexahydrate as a possible PCM for latent heat storage. Solar Energy Materials and Solar Cells, 92(8), pp.891-899.

United Nations Framework Convention on Climate Change (UNFCCC), 2023. COP28 Global Renewables and Energy Efficiency Pledge / Decision Text: Global Stocktake – COP28, Dubai, 30 Nov-13 Dec 2023. Available at: https://www.cop28.com/en/global-renewables-and-energy-efficiency-pledge (Accessed: 20 October 2025)

Wang, F., Zheng, W., Gou, Y., Jia, Y. and Li, H., 2022. Thermal behaviors of energy storage process of eutectic hydrated salt phase change materials modified by Nano-TiO2. Journal of Energy Storage, 53, p.105077.

Wu, X., Lee, J., Varshney, V., Wohlwend, J.L., Roy, A.K. and Luo, T., 2016. Thermal conductivity of wurtzite zinc-oxide from first-principles lattice dynamics–a comparative study with gallium nitride. Scientific reports, 6(1), p.22504.

Xie, N., Niu, J., Wu, T., Gao, X., Fang, Y. and Zhang, Z., 2019. Fabrication and characterization of CaCl2· 6H2O composite phase change material in the presence of CsxWO3 nanoparticles. Solar Energy Materials and Solar

Cells, 200, p.110034.
Xu, X., Dong, Z., Memon, S.A., Bao, X. and Cui, H., 2017. Preparation and supercooling modification of salt hydrate phase change materials based on CaCl2· 2H2O/CaCl2. Materials, 10(7), p.691.
Zhao, Y., Zhang, X., Xu, X. and Zhang, S., 2020. Research progress in nucleation and supercooling induced by phase change materials. Journal of Energy Storage, 27, p.101156.